

See discussions, stats, and author profiles for this publication at: <https://www.researchgate.net/publication/356788899>

Modeling and Control of Mechatronic Aeropendulum

Research · December 2021

DOI: 10.13140/RG.2.2.18357.40161

CITATIONS
0

READS
2,393

1 author:



Arash Marashian

Wärtsilä

22 PUBLICATIONS 50 CITATIONS

SEE PROFILE

Modeling and Control of Mechatronic Aeropendulum

Arash Marashian

marashian.arash@mehr.pgu.ac.ir

*Dynamical Systems & Control (DSC) Research Lab., Department of Electrical Engineering,
Faculty of Intelligent Systems Engineering and Data Science, Persian Gulf University,
75169, Bushehr, Iran*

Abstract

An aeropendulum system built at Dynamical Systems & Control (DSC) Research Lab is presented, identified, and controlled. The system has nonlinear dynamics, which is linearized around the operating point. The identification procedure is done in the frequency domain using the bode diagram. Afterward, using the input shaper, the system's vibration is canceled. In the end, a robust PID controller is designed. All of the above designs are examined using MATLAB real-time simulation and testing. Their results have been reported as well.

1 Introduction

Pendulum is a popular system for designing and testing controllers [1–3]. This system is very convenient to describe the periodic motion. There is some variation of pendulum systems, such as aeropendulum, which consist of a propeller attached to a motor shaft to produce a thrust force in order to move a rod to the desired angle. The inverted pendulum is the other form of this system, which is inherently unstable and is used to model the humanoid robot's dynamics [4]. This system is shown in Fig. 1.

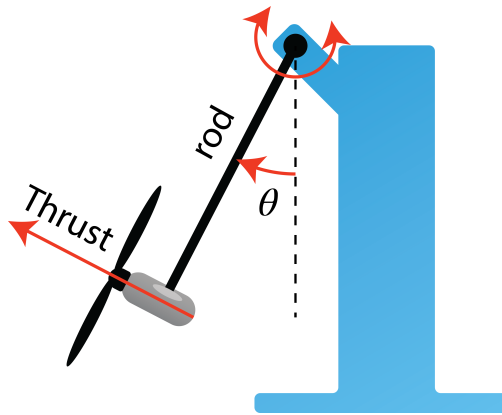


Figure 1: Aeropendulum system.

At first the mathematical nonlinear model of the system is obtained then the linear form of the system is calculated around the operating point. A parameter analysis is reported, which specifies the effect of the parameters values. This will help us to design a suitable system.

The system in the identification part of this project is considered to be gray-box. To obtain an informative data set, we perform an examination that will give us several data-packs. This will help the identification procedure to be more accurate.

In [5], besides the description of an aeropendulum, the proportional-integral-derivative (PID) control and linear-quadratic regulator (LQR) control are presented with comparison in terms of the performance obtained for each controller. In [6], the aeropendulum is presented as a good alternative for a low-cost hands-on experiment with modeling and feedback linearization.

PID controller is very common in the precision industry, which has shown a good result. In this project, we intend to use a robust PID controller as well. However, since aeropendulum systems experience oscillation, we designed an input shaper to reduce this transient behavior. For this cause, a ZVD shaper is presented

Table 1: Aeropendulum system parameters.

	Description
m	Pendulum mass (kg)
l	Pendulum length (m)
d	Distance from pivot to center of mass (m)
c	Viscous damping Coefficient (Nms/rad)
J	Moment of inertia (Kgm^2)
g	Gravity acceleration (m/s^2)
K_m	Gain of propeller (Nm/ μs)

in [7]. On the other hand, as we want to design a robust system, as presented in [8], we will use ZVDD shaper, since it shows a more robust behavior than the others.

2 Mathematical Model

The mathematical dynamics of the aeropendulum system is presented as follows [5]

$$\begin{aligned} \begin{bmatrix} \dot{\theta} \\ \ddot{\theta} \end{bmatrix} &= \begin{bmatrix} 0 & 1 \\ -\frac{mlgd \sin \theta}{J\theta} & \frac{c}{J} \end{bmatrix} \begin{bmatrix} \theta \\ \dot{\theta} \end{bmatrix} + \begin{bmatrix} 0 \\ \frac{K_m}{J} \end{bmatrix} u \\ y &= [0 \quad 1] \begin{bmatrix} \theta \\ \dot{\theta} \end{bmatrix} \end{aligned} \quad (1)$$

where u is the system input, y is the system output and, finally, θ and $\dot{\theta}$ are the system state variables angular displacement and angular velocity, respectively. Note that in (23) one has a nonlinear dynamic in the state space model structure $\dot{x} = f(x, u)$ with the term $\sin \theta$. The system parameters are described in Table 1.

The nonlinear dynamic presented in (1), is linearized around the operating point

$$\frac{\theta(s)}{u(s)} = \frac{K_m/J}{s^2 + (c/J)s + (mlgd/J)} \quad (2)$$

which will be equal to the following using simple calculations

$$\frac{\theta(s)}{u(s)} = \frac{K}{\frac{s^2}{\omega_0^2} + 2\zeta \frac{s}{\omega_0} + 1} \quad (3)$$

in which

$$\omega_0 = \sqrt{\frac{\alpha}{J}}, \quad \zeta = \frac{c}{2\sqrt{\alpha J}}, \quad K = \frac{K_m}{\alpha}, \quad \alpha = mlgd$$

The impact of the three c , m , and l parameters are shown in Fig. 2. As it can be seen, by increasing the mass and the length of the pendulum, the phase margin of the system will be reduced, which informs us not to pick a heavy mass and long rod. On the other hand, increasing the viscous damping coefficient will increase the phase margin.

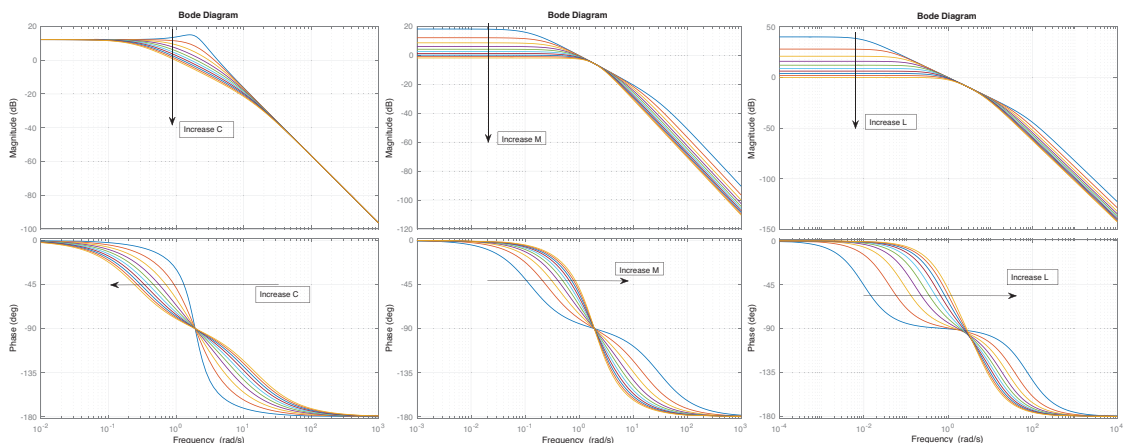


Figure 2: The impact of the parameter variation on the systems bode plot.

3 Actual System

The desired system and its components are shown in Fig. 3. In order to sense the angular position of the rod, we use the CMPS11 sensor. An advantage of this sensor is that it inherently has a Kalman filter, reducing the error of angular computation dramatically, and there is no need to use a computational time in the control loop. We used the Arduino Due as the microprocessor. Since this board is based on a 32-bit ARM core microcontroller, it has an 84 MHz clock speed, which will increase the speed of the controller. Coreless motors are well suited here, as they have a low weight despite their high speed and thrusts. However, they use a high range of current, which will tend us to use a good driver motor that can handle this range of currents. For this reason, we used the Monster Moto Shield driver. These components can be seen in 4.

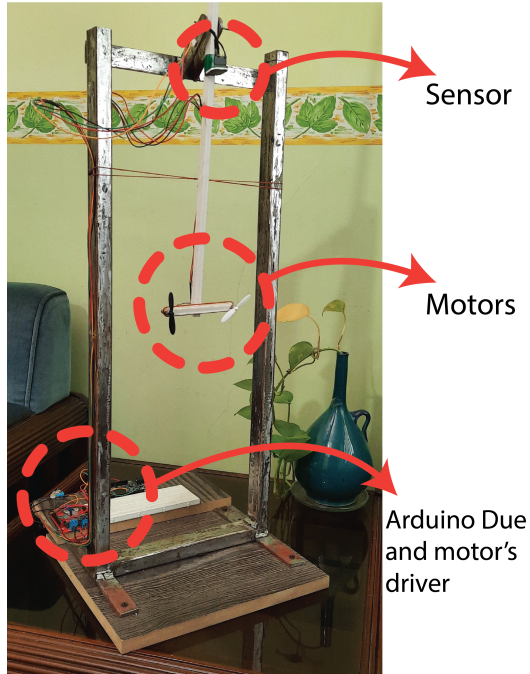


Figure 3: Actual aeropendulum system.

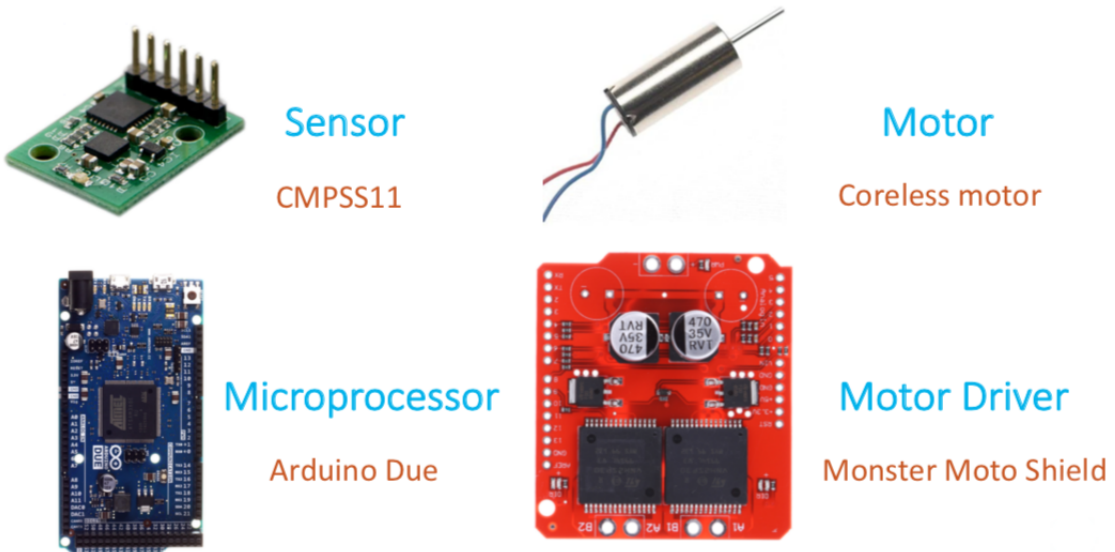


Figure 4: Components has been used in this project.

4 System Identification

In order to identify the system, we have to gain an informative data set. For this reason, we consider six pack of Input-Output data sets, which is illustrated in Fig. 5. This data set is collected using a 100 Hz sampling frequency. The data acquisition procedure that has been used here, is done using the Arduino Library package for Simulink. As it can be seen in 5, we tend to excite the system with sinusoidal input that has a frequency between 0.1 Hz to 3 Hz.

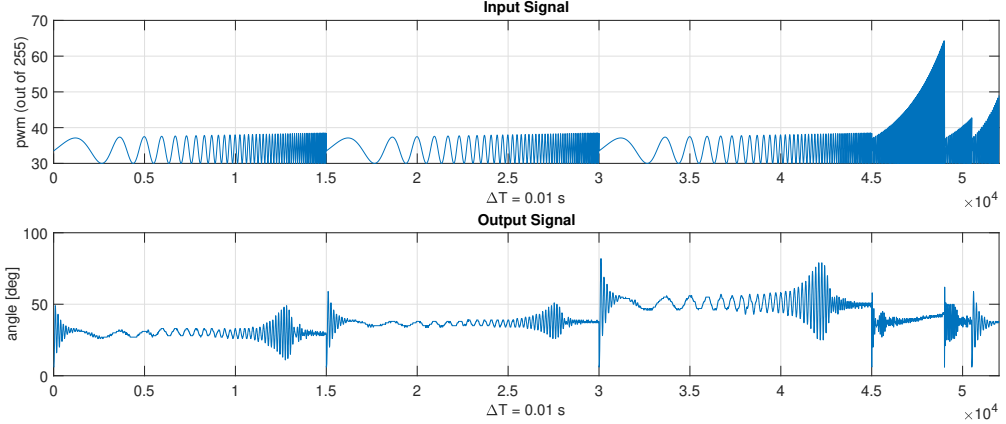


Figure 5: Collected data set for the identification process.

Using `tfeestimate()` in MATLAB, we obtained the frequency response of the system, which is displayed in Fig. 6. It can be seen that after 3 Hz, the bode plot makes no sense. This happens because we did not excite the system in these frequencies. The fitted model is presented in Fig. 6 as well. Here, in order to compensate for the jumps between each pack of data, we used a window size of 1024 and the number of overlap is considered to be 512.

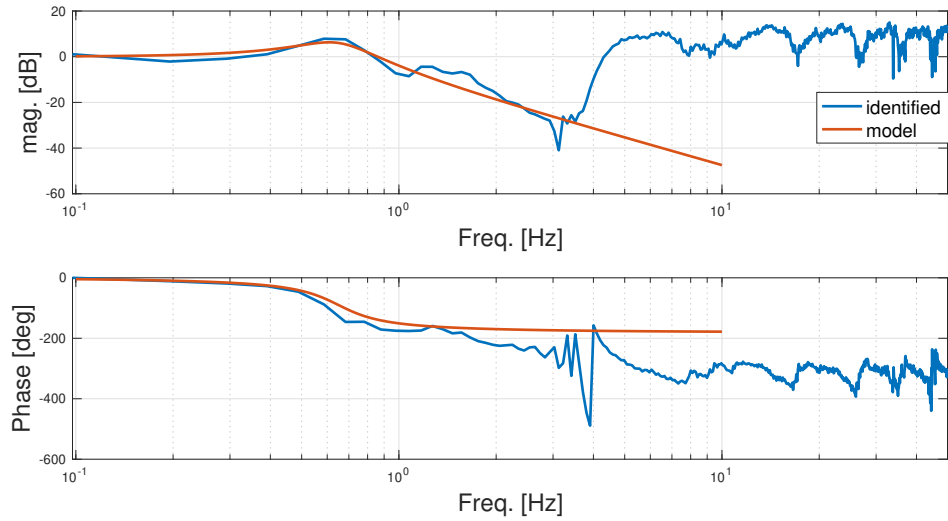


Figure 6: Frequency response of the system.

The fitted model presented in Fig. 6 is

$$G(s) = \frac{\theta(s)}{u(s)} = \frac{K}{\frac{s^2}{4.08^2} + 2(0.25)\frac{s}{4.08} + 1} \quad (4)$$

The constant K , can not be identified as we did not excite the system at low frequencies. In order to calculate this constant, step response analysis is needed, see Fig. 1. the constant K can be calculated as follows

$$K = \frac{\text{steady state of the system}}{\text{steady state of the mode}} = \frac{23}{15} = 1.53$$

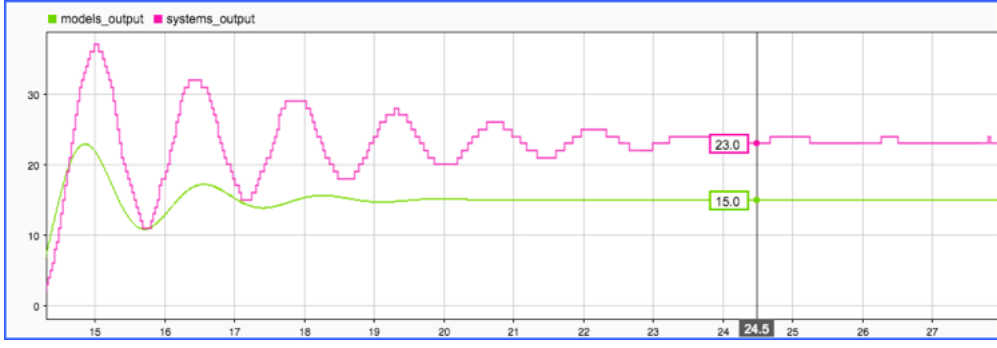


Figure 7: Step response of the system.

5 Pre-filter

In order to reduce the vibration of the system, an input shaper can be used. A robust form of the input shaper is ZVDD which can be described as follows.

$$\text{ZVDD}(s) = \sum_{i=1}^4 A_i e^{-st_i}$$

where

$$\begin{bmatrix} A_i \\ t_i \end{bmatrix} = \begin{bmatrix} \frac{1}{(1+k)^3} & \frac{3k}{(1+k)^3} & \frac{3k^2}{(1+k)^3} & \frac{k^3}{(1+k)^3} \\ 0 & \frac{\pi}{\omega_d} & \frac{2\pi}{\omega_d} & \frac{3\pi}{\omega_d} \end{bmatrix} \quad (5)$$

The parameter k is the overshoot in the step response, and ω_d can be calculated using the time difference between the first two peaks. The impact of the input shaper is presented in Fig. 8. It can be seen that without ZVDD, the system experiences the 15 degrees of overshoot, but by implying the ZVDD, it is reduced to 4 degrees.

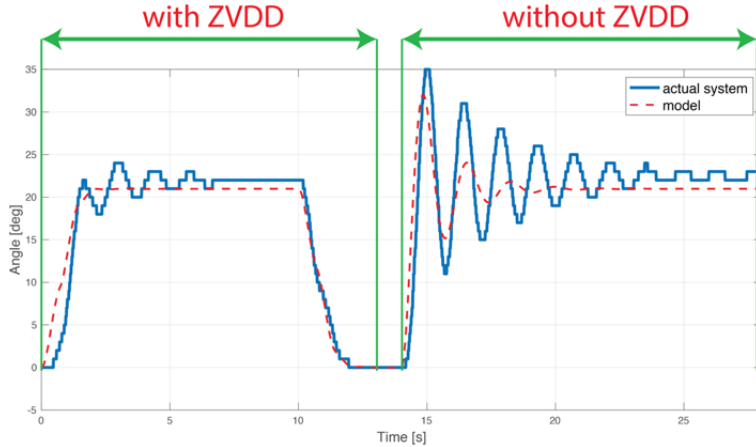


Figure 8: Impact of the ZVDD on the systems transient response.

6 Controller

The control structure that is used in this project is PID.

$$PID = K_p \left(1 + \frac{\omega_i}{s} \right) \left(\frac{\frac{s}{\omega_d} + 1}{\frac{s}{\omega_t} + 1} \right)$$

As the PID controller can inject near 47 degrees of phase, we should seek for the frequency, which has the phase of -167 degrees. In this case, we can have a phase margin of 60 degrees, which will tend us to a robust controller. Considering Fig. 6 and using the ShapeIt software in MATLAB, the chosen bandwidth of the

system is $f_c = 1.5$ Hz. Using the rule of thumb, the parameters of the PID controller described above, are presented

$$K_p = \frac{1}{3|G(s)|_{f_c}} = 0.97, \quad f_i = \frac{f_c}{10} = 0.15, \quad f_d = \frac{f_c}{3} = 0.5, \quad f_t = 3f_c = 4.5 \quad (6)$$

The designed controller increases the systems phase margin to 62.4 degrees, with the modulus margin of 1.8, and the gain margin of infinity. The closed-loop response using the tuned PID and the ZVDD pre-filter is presented in Fig. 9. As it is shown in Fig. 10, in the upper-right figure, we expect that the system reaches the setpoint in near 6 seconds, this can be seen in the actual system presented in Fig. 9.

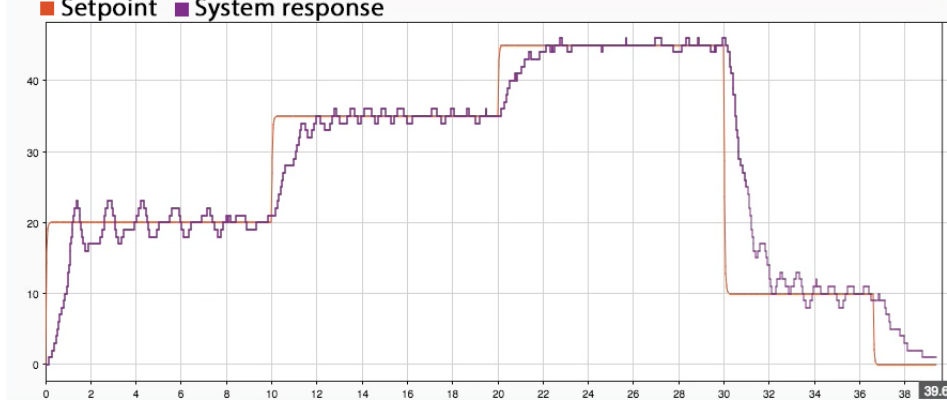


Figure 9: Closed-loop response.

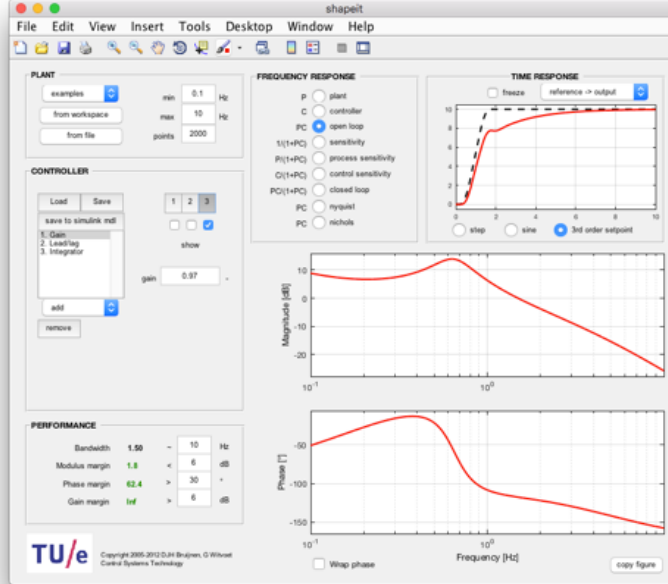


Figure 10: ShapeIt software has been used to designed the controller.

Considering Fig. 11, it will inform us that the disturbance can be damped in nearly 6 seconds. This is tested in the actual system and the results is presented in Fig. 12.

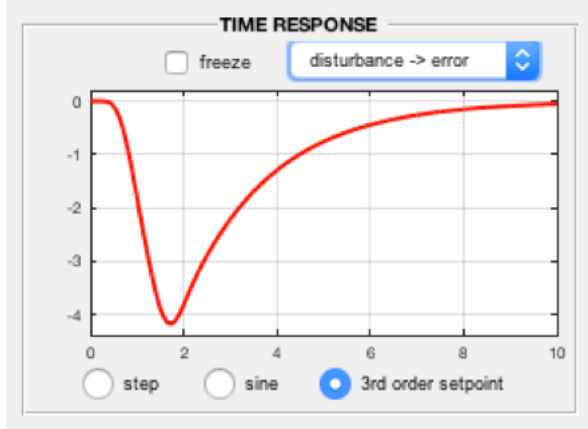


Figure 11: Disturbance rejection presented in ShapeIt software.

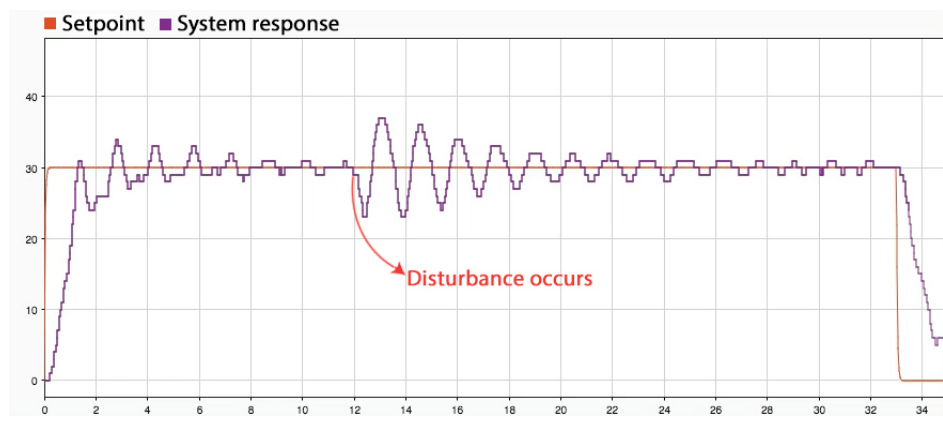


Figure 12: Disturbance rejection in the actual system.

7 Conclusion

In this project, we tend to build a low-cost laboratory device that can be used to test the designed controllers and filters. Firstly, a mathematical equation of the system is presented then the impact of each parameter on the bode plot was investigated. Then considering the results obtained from the previous section, the system was built. Next, the designed system was identified and a second-order transfer function was presented. In order to damp the vibration of the system, an input shaper was composed. A robust PID was tuned to reach the 60 degrees of phase margin. In the end, all the above results were tested on the actual system.

References

- [1] K. Pathak, J. Franch, and S. K. Agrawal, “Velocity and position control of a wheeled inverted pendulum by partial feedback linearization,” *IEEE Transactions on robotics*, vol. 21, no. 3, pp. 505–513, 2005.
- [2] S. Jung and S. S. Kim, “Control experiment of a wheel-driven mobile inverted pendulum using neural network,” *IEEE Transactions on Control Systems Technology*, vol. 16, no. 2, pp. 297–303, 2008.
- [3] J. Yang, H. Lee, J. Hwang, N. Lee, H. Lee, G. Lee, and S. Bae, “A study on the robust control of an inverted pendulum using discrete sliding-mode control,” in *Intelligent Control and Automation*, pp. 456–462, Springer, 2006.
- [4] T. Sugihara, Y. Nakamura, and H. Inoue, “Real-time humanoid motion generation through zmp manipulation based on inverted pendulum control,” in *Proceedings 2002 IEEE International Conference on Robotics and Automation (Cat. No. 02CH37292)*, vol. 2, pp. 1404–1409, IEEE, 2002.
- [5] M. M. Job and P. S. H. Jose, “Modeling and control of mechatronic aeropendulum,” in *2015 International Conference on Innovations in Information, Embedded and Communication Systems (ICIIECS)*, pp. 1–5, IEEE, 2015.
- [6] E. T. Enikov and G. Campa, “Mechatronic aeropendulum: demonstration of linear and nonlinear feedback control principles with matlab/simulink real-time windows target,” *IEEE transactions on education*, vol. 55, no. 4, pp. 538–545, 2012.
- [7] S. Gürleyük and Ş. Cinal, “Robust three-impulse sequence input shaper design,” *Journal of Vibration and Control*, vol. 13, no. 12, pp. 1807–1818, 2007.
- [8] C. Conker, H. Yavuz, and H. H. Bilgic, “A review of command shaping techniques for elimination of residual vibrations in flexible-joint manipulators,” *Journal of Vibroengineering*, vol. 18, no. 5, pp. 2947–2958, 2016.